Confinement: A real-time visualization

Zi Cai,[1] Congjun Wu,[1] and U. Schollwöck[2]

[1]*Department of Physics, University of California, San Diego, California 92093, USA*

[2]*Department of Physics and Arnold Sommerfeld Center for Theoretical Physics, Ludwig-Maximilians-Universität München, D-80333 München, Germany*

(Received 17 January 2012; published 2 February 2012; corrected 7 February 2012)

Due to the mechanism of confinement, as known from quantum chromodynamics, it is difficult to observe individual particles carrying fractional quantum number (e.g., quark with fractional electric charge). A condensed-matter example of fractionalized particles is spinons in quasi-one-dimensional spin systems, which are domain walls in the background of Néel configurations carrying spin-$\frac{1}{2}$. Using the time-evolving block decimation algorithm, we visualize the nontrivial spinon dynamics induced by the confine mechanism in a two-leg spin-$\frac{1}{2}$ ladder. It can be illustrated by a simple single-particle picture of Bloch oscillation, not only qualitatively but also quantitatively. We propose the experimental realization and the real time detection of the spinon dynamics in the ultracold boson systems of ^{87}Rb.

DOI: 10.1103/PhysRevB.85.075102 PACS number(s): 75.10.Pq, 05.70.Ln

I. INTRODUCTION

In quantum chromodynamics, quarks are fundamental particles carrying fractional electric charges. However, interactions between quarks grows linearly with distance due to the mechanism of confinement arising from the SU(3) color gauge theory. Consequentially, quarks are confined into color singlet bound states of baryons and mesons, and thus are difficult to observe. In various condensed-matter systems, there also exist excitations carrying fractional quantum numbers, such as the spinon and holon excitations in one-dimensional (1D) Luttinger liquids,[1] the solitons with half fermion charge in one-dimensional conducting polymers,[2] and the quasiparticle and hole excitations in fractional quantum Hall systems,[3] and the monomer excitations in the dimer model in the triangular lattice.[4] In these systems, fractional excitations are deconfined. Some of them have been experimentally detected.

The phenomenon of confinement emerges in quasi-1D strongly correlated systems such as spin ladders. The "quark" in this case is known as spinon, which is the domain wall interpolating between different ordered regions and usually carries fractionalized spin (spin 1/2). Take an antiferromagnetic spin chain with Ising-like exchange anisotropy for an example; the ground state in this case would be a Néel state with twofold degeneracy, while the spinon can be considered as the elementary excitation separating these two degenerate ground states with opposite staggered magnetization. In a single spin chain, no confinement occurs because a pair of spinons could be separated as far from each other as possible without costing energy. For a two-leg ladder system, even an infinitesimal interchain coupling would induce a potential that increases linearly with distance between the spinons.[5–8] Therefore a pair of fractionalized spinon excitations would be confined into an integral spin-1 excitation: a magnon. Recently, a finite-temperature confined-deconfined crossover has been observed in neutron-scattering experiments for a weakly coupled ladder material $CaCu_2O_3$.[9] The signature of the confinement of spinons can be observed from the energy absorption spectrum for spin flips at various wave vectors. In this paper, we reexamine this old concept from a different perspective, which enables us to visualize the confinement directly through the nonequilibrium dynamics in a cold atom system.

Due to the low dissipation rate and the long coherence times, ultracold atoms in optical lattices have opened exciting possibilities for studying nonequilibrium quantum dynamics of many-body systems.[10–16] On the other hand, it also provides a perfect platform to reexamine classic concepts in condensed-matter or particle physics from a different perspective. One example is the spin-charge separation, which plays a central role in strongly correlated systems.[17,18] Recently, Kollath *et al.*[19] have used the adaptive t-DMRG[20] to study the time evolution of a 1D fermionic Hubbard model in real time, and observed the splitting of local perturbation into separate wave packets carrying charge and spin. In this paper, we study the time evolution of a pair of spinons in a two-leg spin ladder model, and find that the confinement mechanism would lead to nontrivial dynamics of the spinons, which enables us to visualize confinement in real time.

II. CONFINEMENT IN A TWO-LEG SPIN LADDER

Our departure point is a two-leg spin-$\frac{1}{2}$ ladder with easy axis anisotropy along the z axis defined as

$$H = \sum_{i,a} J_{a,\parallel}(S^+_{i,a}S^-_{i+1,a} + \text{H.c.}) + J^z_{a,\parallel}S^z_{i,a}S^z_{i+1,a} - J^z_{\perp}S^z_{i,1}S^z_{i,2}, \tag{1}$$

where $a = 1,2$ is the leg index; $\parallel$ and $\perp$ denote the couplings along the leg and across the rung, respectively. The couplings within legs are antiferromagnetic with the Ising anisotropy ($J^z_{a,\parallel} > 2J_{a,\parallel} > 0$). The rung coupling is chosen as Ising-like and ferromagnetic. The experimental realization of Eq. (1) in ultracold atom systems will be discussed later. Below we will focus on the case of $J_{1,\parallel} \neq J_{2,\parallel}$ which gives rise to the nontrivial dynamics induced by spinon confinement.

Because of the Ising anisotropy and the ferromagnetic rung coupling, the ground state is a Néel state within each leg and with the spins of each rung aligned as shown in

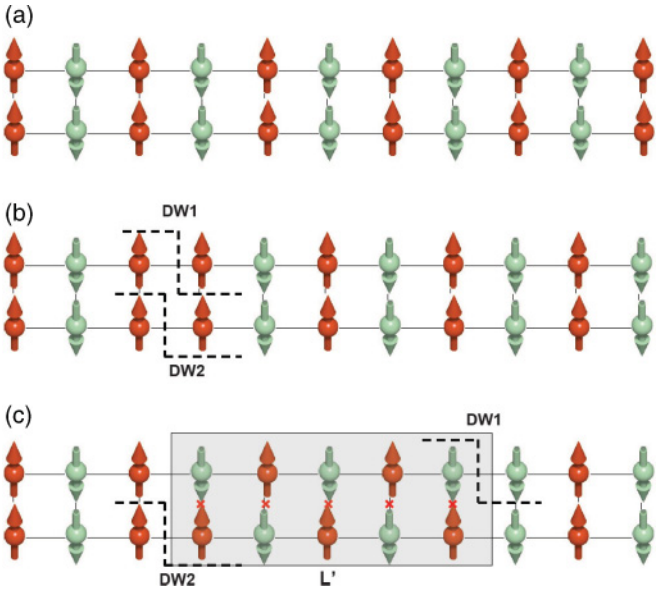

FIG. 1. (Color online) Confinement on the two-leg spin-$\frac{1}{2}$ ladder with Ising anisotropy described by Eq. (1). (a) The classic ground state with Néel ordering along the leg and ferromagnetic ordering along the rung. (b) The classic configuration with $spinon_1$ and $spinon_2$ located at the same position. (c) The mismatch of the locations of $spinon_{1,2}$ gives rise to the energy cost linearly increasing with the mismatch length.

Fig. 1(a).[21] Introducing two spinons in each leg respectively located at the same position cost the domain-wall energy $E_b = \frac{1}{2}(J^z_{1,\|} + J^z_{2,\|})$ as shown in Fig. 1(b). The separation of $spinon_1$ and $spinon_2$ will lead to a mismatch within the rungs between $spinon_1$ and $spinon_2$. This induces a finite string tension between spinons that grows with distance, leading to the confinement,[8] as shown in Fig. 1(c). The transverse spin couplings $J_{a,\|}$ generate spinon dynamics. In the absence of the rung coupling, two spinons move independently with velocities $v_a \propto J_{a,\|}$.[22] In the case of $J_{1,\|} \neq J_{2,\|}$, $spinon_1$ and $spinon_2$ propagate with different velocities, thus become apart eventually. The effective potential between spinons is known as[7]

$$V(r) = k\left|\frac{r}{a}\right|, \quad k \propto J^z_\perp \langle G|S^z_{i,1}S^z_{i,2}|G\rangle, \tag{2}$$

where r is the average distance between these two spinons; a is the lattice constant; $\langle G|S^z_{i,1}S^z_{i,2}|G\rangle$ is taken over the ground state.

III. CONFINEMENT-INDUCED DYNAMICS OF SPINONS

In our numerical simulation, we use the open boundary condition (OBC) and prepare the initial state as both spinons located at the left end of the ladder, i.e., between the first and second sites. Right after the beginning of the evolution, the spinons will be rebounded by the left boundary and propagate toward the left end with a velocity proportional to $J_{a,\|}$. The length of the ladder is set to $L = 20$, long enough for the time scales simulated to exclude finite-size effects. Utilizing the time-evolving block decimation (TEBD) algorithm,[23] we study the time evolution of the many-body wave function from the initial state. Total S^z conservation is used to reduce the computational effort. In the course of real time evolution we take the truncation dimension $\chi = 80$ and time step $\Delta\tau = 0.05$. The convergence is checked by taking larger χ.

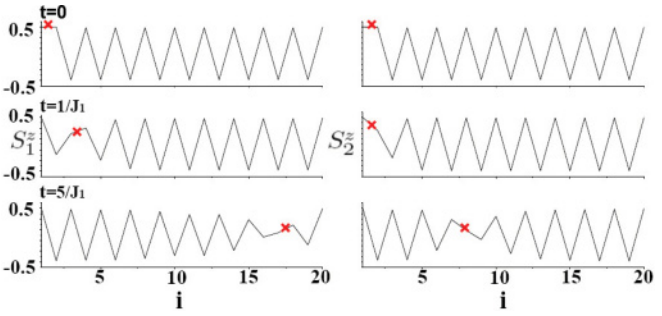

FIG. 2. (Color online) Time evolution of the spinon dynamics with $J^z_\perp = 0$ with the spinon positions marked by the red cross. The spinons in the first (left) and second (right) leg move independently.

The calculated time evolution for the case of $J^z_\perp = 0$ is shown in Fig. 2 in which two spinons are decoupled. The parameter values are taken as $J_{1,\|} = J, J_{2,\|} = 0.5J$, and $J^z_{1,\|} = J^z_{2,\|} = 5J$. To visualize the spinon dynamics, we present the time evolution of the configuration of the expectation value of S_z. The spinons are located at the bonds connecting two sites with the same sign of S_z. During the evolution, two spinons become separated due to their different velocities determined by $J_{a,\|}$. For a clear presentation of the spinon, we define the rectified magnetization $\mathbb{S}_{i,a}$ for each leg as

$$\mathbb{S}_{i,a} = -S^z_{i,a} \times (-1)^i. \tag{3}$$

The location of $spinon_1$ or $spinon_2$ is determined at the bond across which $\mathbb{S}_{i,a}$ changes the sign. The time evolution of the spatial distributions of $\mathbb{S}_{i,a=1,2}$ at $J^z_\perp = 0$ is depicted in Fig. 3(a). Both legs exhibit the propagation of spinons at uniform speeds. The speed of the first leg is larger than that of the second one because $J_{1,\|} > J_{2,\|}$.

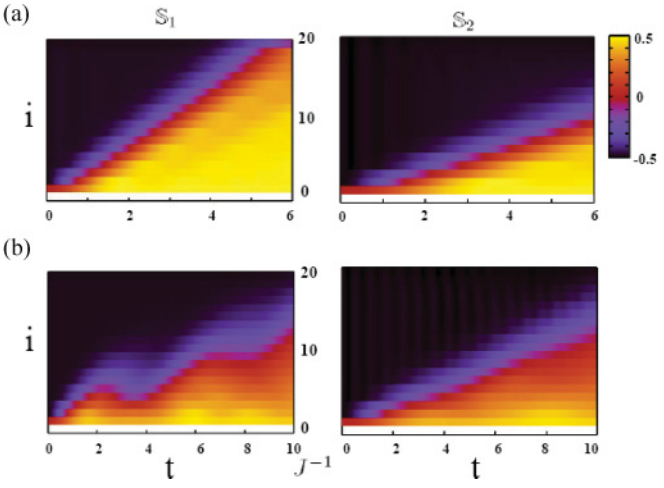

FIG. 3. (Color online) The time evolution of the spatial distribution of $\mathbb{S}_{i,a=1,2}$ for (a) $J^z_\perp = 0$ and (b) $J^z_\perp = J$. They exhibit the propagations and oscillations of the spinons in the first (left) and second (right) legs.

Now we turn on the coupling along the rung; a confinement potential emerges between two spinons. It acts like a "constant" force connecting these two spinons. If we view the spinons as particles, the dynamics of the spinons can be qualitatively understood from a simple two-body picture as follows. Two particles with different initial velocities and masses move in a 1D lattice system and interact with each other via a linear potential. Each particle oscillates around the center of mass (COM) of the system, which continues to do uniform linear motion until it reaches the boundary. This simple picture could be verified qualitatively by our numerical simulation of the spinon dynamics. The time evolution of spatial distribution of $\mathbb{S}_{i,a=1,2}$ at $J_\perp^z = J$ is presented at Fig. 3(b). An oscillation of the $spinon_1$ is observed, while that of $spinon_2$ is not as clear as $spinon_1$. The effective mass of $spinon_2$ is larger than that of $spinon_1$, thus its oscillation amplitude is too small to be visible.

To further verify the two-particle picture quantitatively, we choose $J_{2,\parallel} = 0$, which means $spinon_2$ is localized in its initial position at the boundary. In this case, the two-body problem reduces to a one-body problem of $spinon_1$ in a lattice system under a static magnetic field, which is provided by the rectified spins in the second leg. The time evolution of a spinon within a ferromagnetic spin chain under a constant magnetic field has been studied previously; the dynamics turns out to be a perfect Bloch oscillation.[24] In our case, the confinement "constant" force provided by the static $spinon_2$ plays a similar role of the constant electric field ($E \propto J_\perp^z$), and we expect a similar Bloch oscillation dynamics. It implies that the frequency of the oscillation of $spinon_1$ should be proportional to the interaction strength: $1/T \propto J_\perp^z$, where T is the oscillation period. This relation can be verified numerically, as shown in Fig. 4, where we can find a linear relation between $1/T$ and $J_\perp^z$ for both $J_{1,\parallel} = J$ and $1.5J$. Simulation times were long enough to observe the stability of the oscillation phenomenon.

In a perfect Bloch oscillation, the frequency is determined by the strength of the external field ($J_\perp^z$ in our case), and should be independent of the bandwidth ($J_{1,\parallel}$ in our case). However, we find that the oscillation frequency not only depends on $J_\perp^z$, but is also slightly dependent on $J_{1,\parallel}$, especially for large values of $J_\perp^z$. There are two possible factors contributing to the imperfection of Bloch oscillation. One is the boundary effect. Considering the quantum nature of spinons (wave packets), the boundary begins to influence the dynamics even before the centers of spinons reach the boundary. For larger $J_\perp^z$, the amplitude of the Bloch oscillation A is smaller ($A \propto J_{1,\parallel}/J_\perp^z$), which indicates that the motion of the $spinon_1$ is confined to the boundary, therefore the boundary effect becomes more obvious. This can explain why the deviation becomes larger for bigger $J_{1,\parallel}/J_\perp^z$. The other reason comes from deviations from the linear relations of Eq. (2), which can be considered as a zero-order approximation of the exact interaction between spinons. Actually, on a long length scale, it is possible that higher-order nonlinear modifications such as $1/|r|$ emerge due to the quantum nature of spinons.[8]

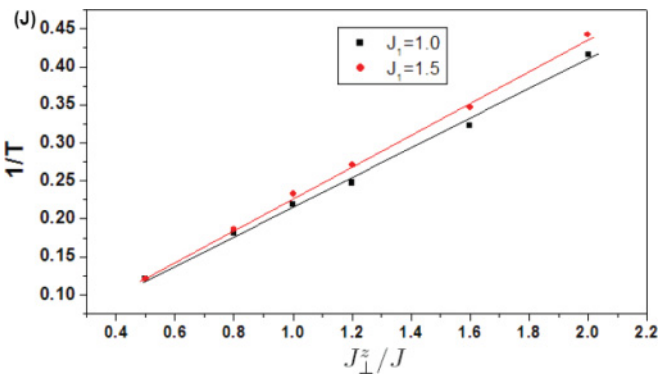

FIG. 4. (Color online) The relation of $1/T$ vs $J_\perp^z$ with parameter values of $J_{2,\parallel} = 0$, and $J_{1,\parallel} = J$ (squares), or $1.5J$ (circles).

IV. EXPERIMENTAL REALIZATION

For an experimental realization of our two-leg spin ladder system in an ultracold atomic superlattice system, one first has to create Néel-ordered chains along the x direction,[25] for example by using ^{87}Rb atoms with two internal spin states $|F = 1, m_F = \pm 1\rangle$. The necessary superexchange interactions of the ultracold atoms can be achieved by the use of a superlattice system.[25–30] In the optical lattice, a typical energy scale for the superexchange coupling J is in the order of kHz, which implies a ms time-scale real time dynamics in our case. By modifying the bias between neighboring lattice sites, both ferromagnetic and antiferromagnetic superexchange interaction can be realized;[25] the orientation of the setup would be as shown in Fig. 5. The two-leg ladder structure is achievable by applying another laser along the y direction to construct a second superlattice structure. In addition, the easy-axis anisotropy is realizable by tuning the interaction $U_{\uparrow\uparrow} = U_{\downarrow\downarrow} \neq U_{\uparrow\downarrow}$,[29,30] or by a periodically modulated lattice.[26] Local addressing techniques as developed recently[31] would be used to create domain walls, e.g., by a global spin flip on one half of the system, as well as for the readout procedure. These techniques, while advanced, are now experimentally established. The arguably most difficult part of the experiment would be to adjust the exchange interaction separately along two different legs. As mentioned above, the exchange interaction can be adjusted by superlattices,[25] but to do this separately on legs 1 and 2, an additional superlattice structure is needed. In fact, antiferromagnetic spin chains have already successfully been simulated, albeit in a different context, namely the Bose-Hubbard model in a tilted optical lattices, where a magnetic domain wall has been observed.[32]

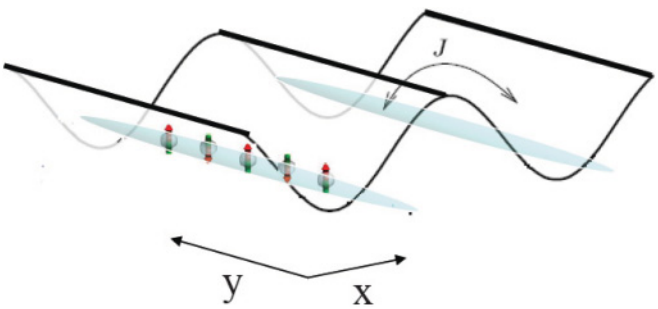

FIG. 5. (Color online) Sketch for the experimental setup of our two-leg spin ladder system.

V. DISCUSSION AND CONCLUSION

In the context of condensed-matter physics, the study of domain-wall motion in magnetic nanowires has attracted considerable theoretical and experimental attention recently due to its potential industrial applications. Manipulation and control of the domain-wall dynamics in magnetic nanowires is known to play an important role in nanomagnetism.[33–35] Most of the theoretical studies in this field are based on the Landau-Lifshitz-Gilbert (LLG) equation.[36,37] Our work is different from previous work in three aspects: (i) we provide a quasiexact calculation of the dynamics of the strongly correlated system by TEBD instead of a semiclassic mean-field approximation; (ii) different from the condensed-matter system where the domain-wall dynamics is closely related with dissipation rate, there is little energy dissipation in our system; (iii) we account for the strong confined interaction between domain walls, which leads to nontrivial dynamics.

Whether in condensed-matter or ultracold atom physics, the control and manipulation of the particles or quasiparticles in the quantum system are of central interest. In this paper, confinement is visualized in real space and its properties are studied via a nonequilibrium process, showing a possible way to investigate and manipulate the motion and interaction of quasiparticles in a dissipationless strongly correlated system. Our work could be helpful for the study of phenomena involving the domain-wall dynamics, such as Walker breakdown[36] and current-driven domain-wall motion.[35]

ACKNOWLEDGMENTS

We are grateful to S. Trotzky for intensive discussions about the experimental realization. Z.C. thanks Lei Wang for numerical help. This work was supported in part by NBRPC (973 program) Grant No. 2011CBA00300 (No. 2011CBA00302). Z.C. and C.W. were supported by NSF Grant No. DMR-1105945 and the AFOSR-YIP program. US was supported by DFG through FOR801.

[1] D. Sénéchal, e-print arXiv:cond-mat/9908262 (to be published).
[2] A. J. Heeger, S. Kivelson, J. R. Schrieffer, and W.-P. Su, Rev. Mod. Phys. **60**, 781 (1988).
[3] R. B. Laughlin, Rev. Mod. Phys. **71**, 863 (1999).
[4] R. Moessner and S. L. Sondhi, Phys. Rev. Lett. **86**, 1881 (2001).
[5] E. Dagotto and T. M. Rice, Science **271**, 618 (1996).
[6] D. G. Shelton, A. A. Nersesyan, and A. M. Tsvelik, Phys. Rev. B **53**, 8521 (1996).
[7] M. Greiter, Phys. Rev. B **66**, 054505 (2002).
[8] M. J. Bhaseen and A. M. Tsvelik, e-print arXiv:cond-mat/0409602 (to be published).
[9] B. Lake, A. M. Tsvelik, S. Notbohm, D. A. Tennant, T. G. Perring, M. Reehuis, C. Sekar, G. Krabbes, and B. Büchner, Nat. Phys. **6**, 50 (2010); M. Greiter, *ibid.* **6**, 5 (2010).
[10] T. Kinoshita, T. Wenger, and D. S. Weiss, Nature (London) **440**, 900 (2006).
[11] K. Winkler, G. Thalhammer, F. Lang, R. Grimm, J. Hecker Denschlag, A. J. Daley, A. Kantian, H. P. Büchler, and P. Zoller, Nature (London) **441**, 853 (2006); A. J. Daley, A. Kantian, H. P. Büchler, P. Zoller, K. Winkler, G. Thalhammer, F. Lang, R. Grimm, and J. Hecker Denschlag, e-print arXiv:cond-mat/0608721 (to be published).
[12] S. Trotzky, Y. A. Chen, A. Flesch, I. P. McCulloch, U. Schollwöck, J. Eisert, and I. Bloch, e-print arXiv:1101.2659 [cond-mat] (to be published).
[13] K. A. Al-Hassanieh, F. A. Reboredo, A. E. Feiguin, I. González, and E. Dagotto, Phys. Rev. Lett. **100**, 166403 (2008).
[14] C. L. Hung, X. B. Zhang, N. Gemelke, and C. Chin, Phys. Rev. Lett. **104**, 160403 (2010).
[15] D. Chen, M. White, C. Borries, and B. DeMarco, e-print arXiv:1103.4662 (to be published).
[16] C. Kasztelan, S. Trotzky, Y. A. Chen, I. Bloch, I. P. McCulloch, U. Schollwöck, and G. Orso, Phys. Rev. Lett. **106**, 155302 (2011).
[17] E. H. Lieb and F. Y. Wu, Phys. Rev. Lett. **20**, 1445 (1968).
[18] G. Baskaram, Z. Zou, and P. W. Anderson, Solid State Commun. **63**, 973 (1987).
[19] C. Kollath, U. Schollwöck, and W. Zwerger, Phys. Rev. Lett. **95**, 176401 (2005); A. Kleine, C. Kollath, I. P. McCulloch, T. Giamarchi, and U. Schollwöck, Phys. Rev. A **77**, 013607 (2008).
[20] A. J. Daley, C Kollath, U Schollwöck, and G Vidal, J. Stat. Mech. (2004), P04005; S. R. White and A. Feiguin, Phys. Rev. Lett. **93**, 076401 (2004); U. Schollwöck, Rev. Mod. Phys. **77**, 259 (2005); Ann. Phys. (NY) **326**, 96 (2011).
[21] T. Giamarchi, *Quantum Physics in One Dimension* (Clarendon, Oxford, 2004).
[22] D. Gobert, C. Kollath, U. Schollwöck, and G. Schütz, Phys. Rev. E **71**, 036102 (2005).
[23] G. Vidal, Phys. Rev. Lett. **91**, 147902 (2003); **93**, 040502 (2004).
[24] Z. Cai, L. Wang, X. C. Xie, U. Schollwöck, X. R. Wang, M. Di Ventra, and Y. P. Wang, Phys. Rev. B **83**, 155119 (2011).
[25] S. Trotzky, P. Cheinet, S. Fölling, M. Feld, U. Schnorrberger, A. M. Rey, A. Polkovnikov, E. A. Demler, M. D. Lukin, and I. Bloch, Science **319**, 295 (2008).
[26] Y. A. Chen, S. Nascimbène, M. Aidelsburger, M. Atala, S. Trotzky, and I. Bloch, Phys. Rev. Lett. **107**, 210405 (2011).
[27] S. Trotzky, Y. A. Chen, U. Schnorrberger, P. Cheinet, and I. Bloch, Phys. Rev. Lett. **105**, 265303 (2010).
[28] J. J. García-Ripoll, M. A. Martin-Delgado, and J. I. Cirac, Phys. Rev. Lett. **93**, 250405 (2004).
[29] L.-M. Duan, E. Demler, and M. D. Lukin, Phys. Rev. Lett. **91**, 090402 (2003).
[30] A. B. Kuklov and B. V. Svistunov, Phys. Rev. Lett. **90**, 100401 (2003).
[31] C. Weitenberg, M. Endres, J. F. Sherson, M. Cheneau, P. Schauß, T. Fukuhara, I. Bloch, and S. Kuhr, Nature (London) **471**, 319 (2011).

[32]J. Simon, W. S. Bakr, R. C. Ma, M. E. Tai, P. M. Preiss, and M. Greiner, Nature (London) **472**, 307 (2011).
[33]S. S. P. Parkin, M. Hayashi, and L. Thomas, Science **320**, 190 (2008).
[34]G. S. D. Beach, C. Nistor, C. Knutson, M. Tsoi, and J. L. Erskine, Nat. Mater. **4**, 741 (2005).
[35]M. Kläui, C. A. F. Vaz, J. A. C. Bland, W. Wernsdorfer, G. Faini, E. Cambril, L. J. Heyderman, F. Nolting, and U. Rüdiger, Phys. Rev. Lett. **94**, 106601 (2005)
[36]N. L. Schryer and L. R. Walker, J. Appl. Phys. **45**, 5406 (1974).
[37]X. R. Wang, P. Yan, J. Lu, and C. He, Ann. Phys. **324**, 1815 (2009).